[15] C. Lanczos, "An iteration method for the solution of the eigenvalue problem of linear differential and integral operators," *J. Research of the National Bureau of Standard,* vol. 45, pp. 255–282, 1950.
[16] R. Fletcher, "Conjugate gradient methods for indefinite systems," in *Numerical Analysis Dundee 1975,* G. A. Watson, Ed. New York: Springer-Verlag, 1976, pp. 73–89.
[17] T. K. Sarkar, "On the application of the generalized bi-conjugate gradient method," *J. Electromagn. Waves Appl.,* vol. 1, no. 3, pp. 223–242, 1987.
[18] M. F. Cátedra, J. G. Cuevas and L. Nuño, "A scheme of analyze conducting plates of resonant size using the conjugate-gradient method and the fast Fourier transform," *IEEE Trans. Antennas Propagat.,* vol. 36, no. 12, pp. 1744–1752, 1988.
[19] W. C. Chew, "Recurrence relation for three dimensional scalar addition theory," *J. Electromagn. Waves Appl.,* vol. 6, no. 2, pp. 133–142, 1992.
[20] J. H. Lin and W. C. Chew, "A comparison of the CG-FFT method and the recursive aggregate T-matrix algorithm," in *IEEE Antennas Propagat. Soc. Int. Symp. Dig.,* 1992, pp. 1591–1594.

Reduced Invasiveness of Noncontact Electrooptic Probes in Millimeter-Wave Optoelectronic Characterization

A. Zeng, S. A. Shah, and M. K. Jackson

***Abstract*—We report time-resolved measurements of the invasiveness of $LiTaO_3$ external probes in millimeter-wave electrooptic sampling. Using external probe tips at varying distances from a coplanar stripline, we show that invasiveness can be reduced in a noncontact configuration at the expense of measurement sensitivity. In the contact configuration, the risetime can be significantly lengthened by dispersion and signal reflection caused by the probe tip.**

I. Introduction

Electrooptic sampling (EOS) has been used in characterization of high-speed electronic devices [1]–[3]. Many of these measurements were made using $LiTaO_3$ external probes. To date there have been a limited number of experimental studies of the invasiveness of $LiTaO_3$ probes. The effects of reflection between the top and bottom interfaces of the $LiTaO_3$ crystal on amplitude measurement has been studied by Frankel *et al.* [4]. The effect of probe-tip-induced dispersion on risetime measurements has been studied by putting a dummy $LiTaO_3$ crystal between the electrical signal generator and the probe site [1]. In both of these studies the $LiTaO_3$ probes were placed in direct contact with the transmission line electrodes and the measurements were performed in the time domain. The invasiveness of external probes has also been studied using internal electrooptic sampling, where a dummy probe was placed in the vicinity of the electrodes of a coplanar stripline driven by a microwave synthesizer [5], [6]. Theoretical studies of the invasiveness of electrooptic probes have been reported [7], [8].

In this paper, we report a study of the invasiveness of external $LiTaO_3$ probes, extending previous measurements to higher frequencies and lower invasiveness. We show that contact electrooptic sampling can lead to measurement error. We also show that noncontact electrooptic sampling provides a more accurate measurement of risetime, at the expense of reduced sensitivity.

Manuscript received February 22, 1995; revised March 20, 1996. This work was supported in part by the Natural Sciences and Engineering Research Council of Canada (NSERC) under individual research grants and networks of centers of excellence (Micronet) programs as well as fellowship support from the University of British Columbia and NSERC.

The authors are with the Department of Electrical Engineering, University of British Columbia, Vancouver, BC V6T-1Z4, Canada.

Publisher Item Identifier S 0018-9480(96)04721-7.

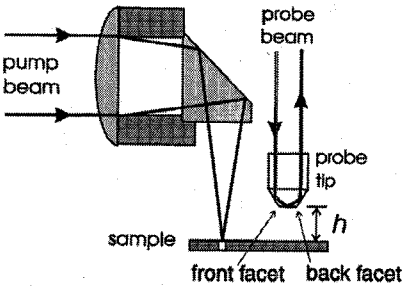

Fig. 1. Schematic of the pump and probe optics. The air gap h between the tip and the sample can be adjusted.

II. Experiment

Electrooptic measurements are made with 150-fs pulses from a mode-locked Titanium-Sapphire laser. The external probe has an inverted pyramid shape, with a $LiTaO_3$ crystal of footprint 200 μm square and thickness 20 μm at the bottom. The arrangement of pump and probe optics and the sampling tip is shown in Fig. 1; the probe is used in a total-internal-reflection configuration, and the probe-sample spacing h can be adjusted. Imaging of interference fringes under the probe tip is used as a indication of probe tip parallelism with respect to the sample surface, which is essential to ensure good contact. The sample is a coplanar stripline with 50-μm-wide electrodes and 5-μm spacing deposited on a 500-μm-thick semi-insulating GaAs substrate. A photoconductive switch incorporated in the transmission line is used to generate step like pulses.

III. Results

In Fig. 2, we show waveforms measured with two different air gaps, and at two different positions of the probe beam in the sampling tip; the probe is approximately 1.5 mm from the photoconductive switch. In Fig. 2(a), we show results for $h = 0$ (contact); the solid line shows the waveform measured with the probe beam positioned near the facet closest to the photoconductive switch, which we will refer to as the front facet. The risetime of the signal is 1.9 ps. The dashed line in Fig. 2(a) shows the waveform measured with the probe beam near the back facet; the risetime in this case is 2.1 ps. In Fig. 2(b), we show similar measurements for an air gap of $h = 10\,\mu$m. The solid line measured at the front facet has a risetime of 1.7 ps, which is the same as the risetime of the signal measured at the back facet, shown by a dashed line.

The differences between the risetimes seen in Fig. 2(a) are not due to the usual dispersion on the undisturbed transmission lines; we have made measurements of risetime at varying distances along the transmission line that show no significant difference in risetime over the same distance. We attribute the lengthening in risetime to the increased dispersion and attenuation introduced by the $LiTaO_3$ probe, which functions as a superstrate. In Fig. 2(a), the feature near 14 ps in the curve measured near the front facet is due to reflection from the back facet of the probe, because of the large mismatch caused by the differing impedances of the transmission lines with and without the $LiTaO_3$ superstrate. The same reflection is not as obvious in the

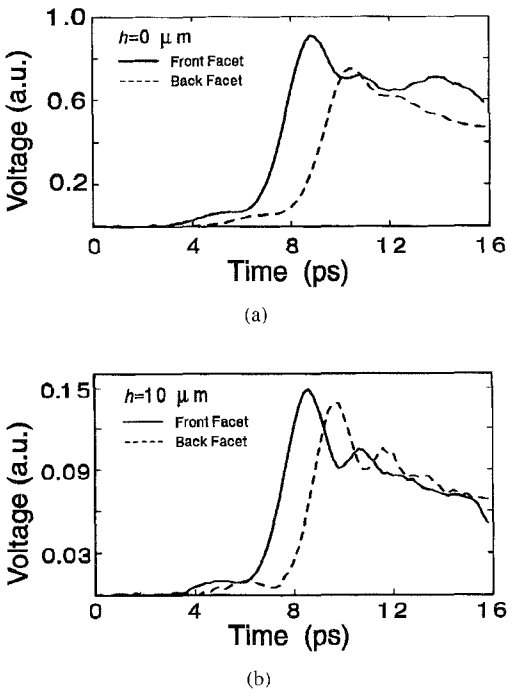

Fig. 2. Contact and noncontact EOS measurements at two probe beam positions in the probe tip: near the front facet (solid lines), and near the back facet (dashed lines). (a) Contact EOS measurements ($h = 0\,\mu$m) and (b) noncontact ($h = 10\,\mu$m) measurements.

measurement near the back facet because the reflection is overlapped with the initial peak due to the small separation between probe spot and the back facet. There is no evidence of a back-facet reflection in either of the noncontact measurements shown in Fig. 2(b). Further comparison of the data of Fig. 2 shows that well-resolved ringing is seen in the noncontact measurement, which is much less evident when in contact. It is interesting to note that when the probe tip is in contact the ringing is still evident, but much more rapidly damped, which is further evidence of probe-tip-induced distortion. The reduced risetime and more clearly resolved features show that the tip-induced distortion of the signal is significantly reduced in the noncontact configuration.

To further quantify the probe-tip-induced dispersion, we made a series of measurements at a distance 1.5 mm from the photoconductive switch with varying air gap h. The risetimes measured are shown in Fig. 3 as a function of air gap from $h = 0$ to approximately 45 μm. The risetime initially decreases with increasing air gap h, and then remains constant within experimental error once the air gap exceeds approximately 20 μm. We performed similar measurements on another sample at a location 3.0 mm from the photoconductive switch, and observed similar results, with risetime decreasing from 3.6 ps when in contact to 3.0 ps with $h = 20\,\mu$m.

Considering the data on dispersion we have presented in Figs. 2 and 3, two different effects are apparent. First, when the tip is in contact, significant dispersion happens as the signals traverses the region under the tip. When the tip is moved away from the surface this dispersion under the tip becomes negligible, but the measured risetime continues to drop with increasing air gap. This second effect can be explained by preferential reflection of high-frequency components at the front probe facet. This interpretation is consistent with the predictions of Conn [8]. Finally, we note that our observations cannot easily be reconciled with the results of [1], where a 200-μm-long $LiTaO_3$ crystal was used as a load in contact with a coplanar stripline. The effect of the load on the transmitted pulse was to lengthen the risetime from 480–520 fs. Considering the much higher bandwidth of

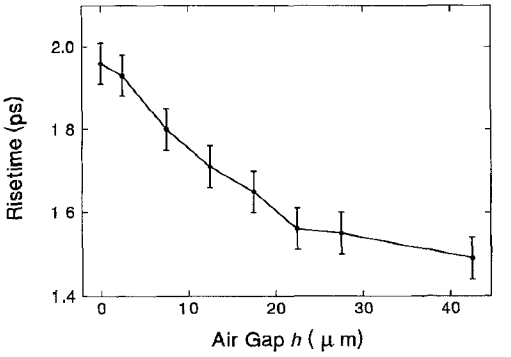

Fig. 3. Measured risetimes as a function of air gap h

these pulses, the effective dispersion caused by the tip is much lower than what we observe. The observations of [1] could be attributed to imperfect contact between the $LiTaO_3$ crystal and the transmission lines. We also note that the delay induced by the load in [1] is much smaller than expected given the high dielectric constant of $LiTaO_3$.

Having discussed the effect of air gap on dispersion, we now examine its effect on sensitivity, which will place a lower limit on tip invasiveness. In Fig. 4 the solid line connects the squares, which show the peak amplitudes of the time-resolved waveforms measured at varying air gaps, as a function of h. The amplitudes have been normalized to the value at 2.5 μm; this point was chosen instead of 0 μm because the measured amplitude in contact is difficult to reproduce exactly due to changes in the pressure with which the tip contacts the transmission line. Starting from $h = 0$, the signal initially drops dramatically with increasing air gap h, but then less quickly once the air gap is greater than approximately 20 μm. We also plot in Fig. 4 a dashed line that connects the diamonds showing the EOS signal measured when a low-frequency calibration voltage is applied to the transmission lines. This approach is often used to allow absolute voltage calibration of measured EOS waveforms; the accuracy of this approach depends upon the sensitivity to the low- and high-frequency signals being the same. From Fig. 4 it is apparent that the sensitivities are very similar for air gaps below approximately 40 μm. For larger air gaps a discrepancy between the two curves is seen, indicating that absolute voltage calibration cannot be maintained. We attribute the different dependence on h for large air gaps to a difference in the fringing field distributions. Because the time-resolved signal contains high-frequency components, it will be more confined to the vicinity of the transmission line electrodes than the low-frequency calibration signal.

To compare our results with those of previous workers, in Fig. 4 we also show experimental data of [7] (triangles) and simulation results of [8] (circles). We have also normalized these data to the values at 2.5 μm. The data of [7] were measured with a low-frequency calibration signal; they are not obtained from time-resolved measurement. The sample was a coplanar waveguide with 4-μm center electrode width and 13-μm spacing. The data of [7] decrease with distance at a rate that is nearly constant and similar to what we see at small h; however, there is no obvious sign of the break point seen in our data. This may be due to the differing fringing field pattern of a coplanar waveguide compared to the coplanar stripline. In addition, the electrode spacing used in [7] is greater than in our sample; this might shift a break point to air gaps greater than those used in [7]. The theoretical predictions of [8] shown in Fig. 4 are for a coplanar waveguide with 15-μm center electrode width and 10-μm spacing; it is interesting to note that these data show a break point similar to that seen in our data. The origin of the discrepancy between the data for comparable coplanar waveguides from [7] and [8] is not clear.

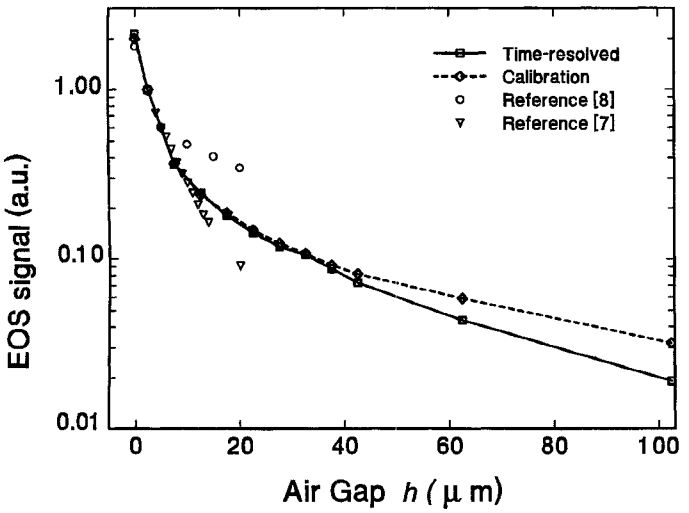

Fig. 4. EOS sensitivity as a function of air gap h. The solid and dashed lines connect the points shown by squares and diamonds, for time-resolved and calibration signals, respectively. The triangles and the circles are the data of [7] and [8], respectively.

IV. Summary

We have studied invasiveness and sensitivity of $LiTaO_3$ external probes for electrooptic sampling of millimeter-wave circuits and devices. Our measurements show two effects that contribute to distortion of the measured signals. The first is dispersion on the coplanar stripline caused by the presence of the $LiTaO_3$ superstrate. However, even once this dispersion is insignificant, pulse distortion is observed that we attribute to frequency-dependent signal reflection at the front probe facet. Both of these distortions can be reduced by using a noncontact arrangement with an air gap between the tip and the transmission line.

References

[1] J. A. Valdmanis, "Electro-optic measurement techniques for picosecond materials, devices, and integrated circuits," in *Measurement of High-Speed Signals in Solid State Devices,* R. B. Marcus, Ed. San Diego: Academic, 1990, pp. 136–219.

[2] A. Zeng, M. K. Jackson, M. Van Hove, and W. De Raedt, "On-wafer characterization of $In_{0.52}Al_{0.48}As/In_{0.53}Ga_{0.47}As$ modulation-doped field-effect transistor with 4.2 ps switching time and 3.2 ps delay," *Appl. Phys. Lett.,* pp. 262–263, 1995.

[3] M. Y. Frankel, J. F. Whitaker, and G. A. Mourou, "Optoelectronic transient characterization of ultrafast devices," *IEEE J. Quantum Electron.,* pp. 2313–2324, 1991.

[4] M. Y. Frankel, J. F. Whitaker, G. A. Mourou, and J. A. Valdmanis, "Experimental characterization of external electrooptic probes," *IEEE Microwave Guided Wave Lett.,* pp. 60–62, 1991.

[5] W. Mertin, C. Roths, F. Taenzler, and E. Kubalek, "Probe tip invasiveness at indirect electro-optic sampling of MMIC," in *'93 IEEE MTT-S Int. Microwave Symp. Dig.,* 1993, pp. 1351–1354.

[6] W. Von Wendorff, G. David, U. Dursum, and D. Jager, "Frequency domain characterization of a GaAs coplanar waveguide up to 40 GHz by electro-optic probing," in *Conf. Proc. LEOS '92,* 1992, pp. 119–121.

[7] T. Nagatsuma, T. Shibata, E. Sano, and A. Iwata, "Non-contact electro-optic sampling system in subpicosecond regime," in *IEEE Instrument. Measure. Tech. Conf. '90,* 1990, pp. 152–158.

[8] X. Wu, D. Conn, J. Song, and K. Nickerson, "Invasiveness of $LiTaO_3$ and GaAs probes in external E-O sampling," *J. Lightwave Technol.,* pp. 448–454, 1993.

Analysis of Microstrip Discontinuities Using the Spatial Network Method with Absorbing Boundary Conditions

Dragos Bica and Benjamin Beker

***Abstract*—In this paper it is shown that spatial network method (SNM) can be formally derived as a finite differencing scheme, which ensures that the necessary stability and convergence conditions are met. For the first time, Mur and Higdon second-order absorbing boundary conditions (ABC's) have been used in conjunction with SNM. It has been found that the Higdon second-order ABC's perform better than the Mur algorithm for guided wave problems with inhomogeneous substrates. Finally, it is shown that SNM can successfully be employed for the analysis of planar and three-dimensional (3-D) microstrip discontinuities in open or shielded environments.**

I. Introduction

During the past decade, the interest in microstrip discontinuities has substantially increased, as can be seen from the growing number of reported research activity on the subject [1]–[5], [12], and [13]. The driving factors behind this trend are increasing frequencies of operation and the continuing need for more accurate design methods for microwave integrated circuits (MIC's). Some microstrip discontinuities, such as steps and bends are due to the interconnects of various MIC's. Others, such as tuning stubs or resonant strips, are used to achieve specific functionality.

Several methods have already been employed for the study of microstrip discontinuities. Green's function based methods, such as the integral equation in spectral domain method [1] or the time domain method of lines [2], have been used to characterize planar discontinuities (open ends, stubs, gaps, steps in width) as well as full 3-D problems such as vias and air bridges [3]. Compared against experimental data, these methods offer very accurate numerical results. The aforementioned methods provide the frequency response of the discontinuity, taking into account the boundary conditions which are built into the Green's functions. However, for complex, nonplanar geometries and for inhomogeneous substrates, such methods are difficult to implement, and volumetric methods are often used instead.

Examples of volumetric methods are the finite difference time domain (FDTD) technique, transmission line matrix method (TLM), and spatial network method (SNM). All of them have been used in the study of microstrip discontinuities. The TLM method, in its frequency domain form, has been used to calculate the S-parameters of transmission line interconnects such as vias and air bridges [4]. The FDTD method has been applied to the study of step, open end, and gap microstrip discontinuities [5].

Time domain differential equation methods can easily accommodate closed boundary conditions associated with shielded structures, but they do not have the inherent ability to simulate the open boundary conditions. To overcome such limitations, several absorbing boundary conditions (ABC's) have been proposed [6]–[8], mostly for the FDTD method, and more recently for TLM [9]. The ABC's have low numerical reflectivity (<-25 dB) if used within appropriate limits, as shown in [8]. The errors introduced by the ABC's can be minimized

Manuscript received June 11, 1995; revised March 20, 1996. This work was supported in part by the US Army Research Office under Grant DAAL03-92-G-0275.

The authors are with the Department of Electrical and Computer Engineering, University of South Carolina, Columbia, SC 29208 USA.

Publisher Item Identifier S 0018-9480(96)04722-9.